FACTA UNIVERSITATIS
Series: **Mechanical Engineering**
https://doi.org/10.22190/FUME220404027S

Original scientific paper

THERMAL BUCKLING AND BENDING ANALYSES OF CARBON FOAM BEAMS SANDWICHED BY COMPOSITE FACES UNDER AXIAL COMPRESSION

Babak Safaei[1,2], Emmanuel Chukwueloka Onyibo[1], Dogus Hurdoganoglu[1]

[1]Department of Mechanical Engineering, Eastern Mediterranean University, Famagusta, Turkey
[2]Department of Mechanical Engineering Science, University of Johannesburg, Gauteng, South Africa

Abstract. *The bending and critical buckling loads of a sandwich beam structure subjected to thermal load and axial compression were simulated and temperature distribution across sandwich layers was investigated by finite element analysis and validated analytically. The sandwich structure was consisted of two face sheets and a core, carbon fiber and carbon foam were used as face sheet and core respectively for more efficient stiffness results. The analysis was repeated with different materials to reduce thermal strain and heat flux of sandwich beams. Applying both ends fixed as temperature boundary conditions, temperature induced stresses were observed, steady-state thermal analysis was performed, and conduction through sandwich layers along with their deformation nature were investigated based on the material properties of the combination of face sheets and core. The best material combination was found for the reduction of heat flux and thermal strain, and addition of aerogel material significantly reduced thermal stresses without adding weight to the sandwich structure.*

Key words: *Sandwich beam, Heat flux, Buckling, Total deformation, Finite element analysis*

1. INTRODUCTION

Sandwich composite structures are made of two thin, rigid skin layers divided by a thicker, softer core as stated by Darzi et al. [1]. Gay and Suong [2] stated that, sandwich

[*]**Received:** April 04, 2022 / Accepted May 23, 2022
Corresponding author: Babak Safaei
Department of Mechanical Engineering, Eastern Mediterranean University, Famagusta, North Cyprus via Mersin 10, Turkey
Department of Mechanical Engineering Science, University of Johannesburg, Gauteng 2006, South Africa
E-mail: babak.safaei@emu.edu.tr

structures were created when two thin facings or skins were bonded or welded together on a lighter core that kept the two skins apart. The core increased the panel's bending stiffness and resistance to buckling loads [3,4]. They also found that sandwich structures had fewer lateral deformations, more buckling resistance, and higher natural frequencies than other types of structures. Douville and Grognec [5] showed that sandwich structures were employed in a wide range of industrial applications due to their desirable combination of light weight and strong mechanical qualities. Therefore, steel is commonly used for the skins [6,7]. Hence, Commonly used materials in the core are metallic foams and polymers [8–10]. Rigid-foam core is commonly used and has moderate strength and stiffness [11]. Moreover, one of the common cores used in sandwich panels is a honeycomb [12–14]. In general, sandwich structures are preferred over traditional materials due to their high corrosion resistance [15] and low thermal and acoustic conductivity [16,17]. The high thermal expansion coefficient of aluminum honeycomb sandwich constructions limits their use in thermal management systems [18]. The behavior and failure modes of sandwich structures in flexure have been observed in a variety of studies [17,19–21]. A sandwich structure can fail due to a variety of damage mechanisms, including tensile failure/skin compressive [22], local skin wrinkling [23,24], and core indentation failure [25,26]. The sensitivity of nap-core sandwich, a unique type of structural composite with different characteristics, was studied by Ha et al. [27]. McCormack et al. [28] studied the failure of sandwich beams with metallic foam cores. Ha et al. [29] studied the behaviors of nap-core sandwiches, with a particular emphasis on the effect of symmetry in nap cores.

In thermal applications, heat conduction and heat flux in sandwich beams has been experimented. Non-Fourier heat conduction was investigated in a sandwich panel with a cracked foam core by Fu et al. [30]. Under a high-temperature environment, the vibration properties of a carbon nanotube-reinforced sandwich curved shell panel were explored by Mehar and Kumar Panda [31]. Sun et al. [32] investigated the convective cooling efficiency of a sandwich panel with a hierarchical corrugated core heated from face sheets and cooled actively through the core. Onyibo and Safaei [33] applied finite element analysis to honeycomb sandwich structures. Su et al. [34] investigated the thermal insulation performance of structural insulated panels (SIPs) with glass fiber-reinforced polymer (GFRP) surfaces. Moradi-Dastjerdi and Behdinan [35] presented a smart multifunctional sandwich plate with a central lightweight porous layer, two intermediate polymer/graphene nanocomposite layers, and two piezoceramic active faces. Zhang et al. [36] proposed an energy harvester that used an arc-shaped piezoelectric sheet to scavenge rotational energy from rotating devices. Zhao et al. [37] proposed a multifunctional carbon fiber honeycomb sandwich structure (MCFHS). Safaei et al. [38] presented an analytical solution based on molecular mechanics model to estimate the elastic critical axial buckling strain of chiral multi-walled carbon nanotubes (MWCNTs). Using experimental, theoretical, and numerical simulation methodologies, Chen et al. [39] investigated the heat transmission mechanism and thermal insulation performance of fabricated C/SiC corrugated LCSP. Safaei et al. [40] explored the thermoelastic responses of sandwich plates with porous polymeric core and proposed ultra-lightweight engineering structures of sandwich plates with one porous polymeric core and two carbon nanotube (CNT)/polymer nanocomposite outer layers. Asmael et al. [41] reviewed the ultrasonic machining of carbon fiber–reinforced plastic composites.

According to the law of vibration, everything (components and structures) is in constant motion, vibrating at a given frequency. Safaei [42] investigated the damped vibrational behavior of a lightweight sandwich plate subjected to a periodic force over a short period of time. Liu et al. [43] examined the nonlinear forced vibrations of functionally graded materials (FGMs). Hadji and Avcar [44] investigated free vibration of a square sandwich plate with functionally graded (FG) porous face sheets and an isotropic homogenous core under different boundary conditions. Li et al. [45] theoretically and experimentally studied the nonlinear vibrations of fiber-reinforced composite cylindrical shells (FRCCSs) with bolted joint boundary conditions. Liu et al. [46] developed a novel method for solving nonlinear forced vibrations of functionally graded (FG) piezoelectric shells in multi-physics fields. However, there have been many studies on nonlinear vibration behaviors of various materials [47-54]. The nonlinear forced vibration behaviors of third-order shear deformable nanobeams in the presence of both surface stress and surface inertia due to high surface to volume ratio were investigated by Sahmani et al. [55]. Yang et al. [56] carried out free vibration evaluations on FG graphene nanoplatelet-reinforced composite (FG-GPLRC) arches in both in-plane and out-of-plane. Katariya et al. [57] used higher-order shear deformation theory to construct a generic mathematical model for evaluating the bending and vibration responses of skew sandwich composite plates. Enhanced donnell nonlinear shell theory and Maxwell static electricity/magnetism equations were used by Liu et al. [58] to construct a coupled nonlinear model for composite cylindrical shells to examine nonlinear forced vibrations in multi-physics fields. Moradi-Dastjerdi and Behdinan [59] used an innovative and reliable approach to investigate the free vibration behaviors of multifunctional smart sandwich plates (MSSPs).

Buckling is one of the major failure causes of machine elements; therefore, buckling loads should be considered in designs. Bažant and Beghini [60] showed that sandwich shell failures caused by skin, core, and interface fracturing were often associated with instability and as a result, it was difficult to distinguish among delamination, fracturing, damage, buckling, face wrinkling and scaling. However, based on the type of loading, various buckling forms could occur, which can be global or local [61,62]. Zhao [63] investigated new buckling characteristic equation for sandwich pipelines. Alhijazi et al. [64] analyzed the elastic properties of luffa and palm natural fiber composites (NFCs) with epoxy and ecopoxy matrixes, taking fiber volume fractions into account. Fan et al. [65] investigated the thermal post buckling characteristics of porous composite nanoplates. Grygorowicz et al. [66] studied the elastic buckling of a three-layered beam with a metal foam core using analytical and numerical approaches. Ansari et al. [67] studied the pull-in instability properties of hydrostatically and electrostatically actuated circular nanoplates, taking into account the influence of surface stress. Fattahi and Safaei, [68] studied the buckling properties of nanocomposite beams reinforced with single-walled carbon nanotubes (SWCNTs). Liu et al. [69] used a size-dependent numerical solution methodology to investigate nonlinear buckling and post buckling of cylindrical micro sized shells made of checkerboard. Nonlinear buckling of elastically supported functionally graded graphene platelet-reinforced composite (FG-GPLRC) was analytically predicted by Yang et al. [70]. Under temperature conditions, Yang et al. [71] performed an analytical investigation on the asymmetric static and dynamic buckling of a pinned-fixed FG-GPLRC. Safaei et al. [72] performed high-precision thermal and mechanical buckling analyses on UD porous sandwich plates with FG-CNT cluster-reinforced nanocomposite outer layers resting on elastic foundations. Magnucki and Magnucka-Blandzi [73] developed an analytical model for sandwich structures using a rectangular plate as an example. Sahmani and Aghdam [74] studied the size-dependent buckling and post buckling characteristics of microtubules embedded in cytoplasm under axial compressive load using the nonlocal strain gradient theory of elasticity, which included both nonlocality and strain gradient size dependency. This was done within the framework of a refined orthotropic shell theory with hyperbolic distribution of shear deformation. Yunliang and Junping [75] studied bifurcation point buckling and extreme point buckling of sandwich structures. Sahoo et al. [76] investigated the finite element solutions of thermal buckling load values of graded sandwich curved shell structures using a higher-order kinematic model that included shear deformation effect. Avilés and Carlsson [77] developed an elastic foundation model for analysis of the local buckling behavior of foam core sandwich columns containing a through-width face/core debond. Also, there have been numerous investigations on nonlinear buckling [78–80], size-dependent buckling, and bending behaviors [81–84]. Jasion et al. [85] investigated the global and local buckling–wrinkling of the face sheets of sandwich beams and sandwich circular plates using computational and experimental methods. Moreover, Léotoing et al. [86] presented the first implementation of a revolutionary unified sandwich model considering closed-form solutions for both global and local buckling. In the presence of surface stress impact, Fan et al. [87] predicted the shear buckling characteristics of skew nano-plates composed of a FGM. Sahmani and Aghdam [88] investigated the size-dependent buckling and post buckling responses of hybrid FG nanoshells integrated with surface-bonded piezoelectric nanolayers using a refined exponential shear deformation shell theory in conjunction with nonclassical Eringen's nonlocal elasticity theory. Under in-plane hydrostatic and uniaxial compression, elastic buckling of regular hexagonal thin sheets made of homogenous and isotropic materials with internal, translational and rotational elastic edge supports were studied by Ghanati and Safaei [89].

However, bending of a slender structural element characterizes its behavior under an external load applied perpendicularly to a longitudinal axis of element. Furthermore, Yan et al. [90] predicted the bending stiffness, peak load and initial failure load of sandwich structures. Mehar and Panda [91] numerically evaluated the deflection behaviors of carbon nanotube-reinforced composite plates using finite-element method and validated the accuracy of results using three-point experimental bending test data. Barbaros et al. [92] carried out a review on FG porous nanocomposite materials considering manufacturing, application, and mechanical characteristics. Liu et al. [93] investigated the impact responses of shear deformable sandwich cylindrical shells with two face layers and a FG porous core. Aldakheel and Miehe [94,95] investigated coupled thermo-mechanical strain gradient plasticity theory taking into account micro- structure-based size effects. Chen [96] used FEM to investigate the collapse behaviors of corrugated cross section beams subjected to three-point bending. Zhao et al. [97] reviewed the mechanical properties of graphene and graphene composites. Wang et al. [98] proposed a novel multilevel modeling approach for calculating the Young's modulus of polymers reinforced with graphene nanoplatelets. Zhang et al. [99] studied the bending strength, stiffness, and energy absorption of a corrugated sandwich composite structure. Few research works have been carried out on natural fiber composites [100,101]. Mehar and Panda [102] conducted deflection analysis to investigate the effect of MWCNT reinforcement on the rigidity of sandwich curved panels. Sahmani and Aghdam [103] estimated the Young's modulus and Poisson's ratio of nano porous biomaterials with refined truncated cube cells. The effect of adding calcium carbonate nanoparticles (NPs) to cement plast on mechanical characteristics was experimentally explored by Safaei et al. [104]. Li et al. [105] investigated vibro-impact resistant performance of fiber reinforced composite (FRC) plates with polyurea coating (PC) under four-edge elastic constraints. Seong et al. [106]

applied bending mechanism to determine the control parameters of core shear stress and found that, according to analytic calculations, the shear stress of core could be greatly decreased by increasing clearance. Under the impact of mechanical loading and heat field, the frequency, deflection, and stress values of carbon nanotube-reinforced sandwich plate structures were numerically investigated by Mehar et al. [107]. Fattahi et al. [108] presented an experimental investigation on the effect of nanoparticle volume fraction on the elastic characteristics of a polymer-based nanocomposite and obtained comparable results to other existing theoretical models. Moreover, Sivaram [109] improved the strength and mechanical properties of aluminum materials by the inclusion of polypropylene foam sheets. Hu and Wang [110] created a thermal–mechanical analysis model to characterize thermal shock behaviors of auxetic honeycomb core ceramic sandwich structures (CSSs). Daouas et al. [111] investigated thermal performance of walls under optimal conditions. Wang et al. [112] derived an exact analytical solution for steady-state heat transfer in FG sandwich slabs under convective-radiative boundary conditions. Geoffroy et al. [113] studied 3D printed sandwich materials filled with hydrogels at extremely low heat release rates. Safaei et al. [114] used FEM to examine the effect of static and harmonic loads on honeycomb sandwich beams.

In this paper, the flexural strength of sandwich beams was improved, heat flux and temperature at which sandwich structures buckle were determined using finite element analysis (commercial software ANSYS). In a connected linear buckling analysis of sandwich beams, the load factor on the static load causing buckling was assessed, the critical buckling load and bending behavior of carbon fiber strut imbedded in sandwich core was determined. In general, sandwich beam heat transfer and thermal strain at corresponding temperature were investigated and compared with added silica aerogel material.

2. Problem Objective

In this paper, the analysis of buckling caused by thermal expansion in a sandwich beam was presented for simply supported sandwich beams under axial compression and the critical buckling force and buckling mode shapes were investigated. Furthermore, the bending deformation of cantilever sandwich beams with different imbedded carbon fiber materials was studied and results were compared with analytical calculations. In addition, the rate of heat conduction of the sandwich was analyzed to reduce the heat flux and temperature induced stresses and make it a favorable thermal insulator.

2.1 Geometry and Finite Element Model

The geometry of sandwich beam solid model structure was used to investigate bending and critical bucking load, while carbon foam core was applied to analyze heat flux and thermal stresses of a given thickness using finite element analysis. The advantages of sandwich solid model are short computational time, good adhesion properties and more reliable results when compared to analytical solution. Fig. 1(a) shows the Solidworks commercial software design of 8 cylindrical bar struts of 1.5 mm diameter and 10 mm spacing. Fig. 1(b) shows carbon fiber strut imbedded in the core in order to improve sandwich axial compression and Fig. 1(c) depicts rectangle shape strut inserted in the core for absorbing bending stresses in sandwich beams. Furthermore, Fig. 1(d) depicts the sandwich with added aerogel layers. Lastly, Table 1 shows the dimensions of the used sandwich beam.

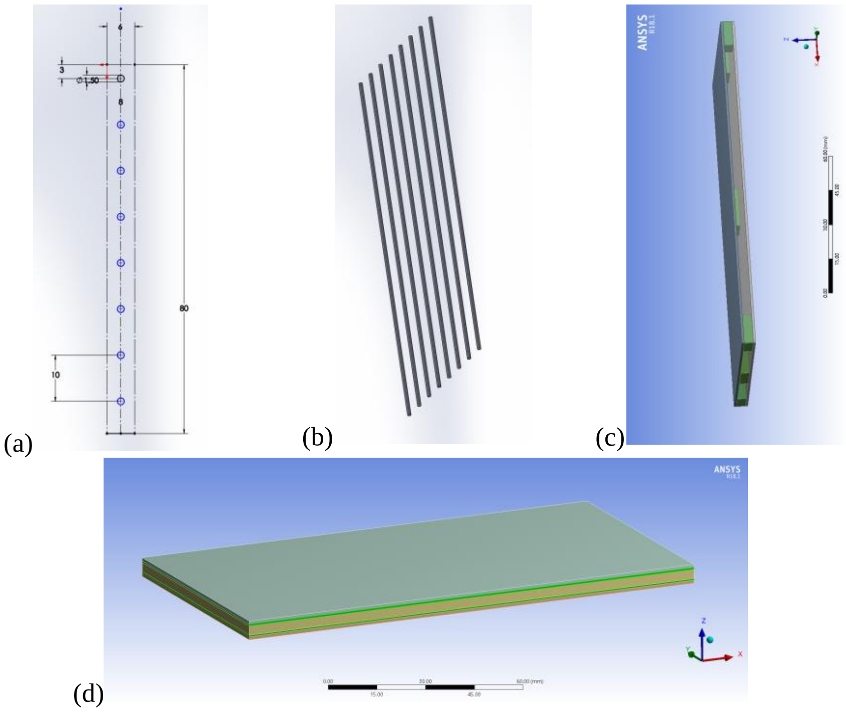

Fig. 1 Geometry of sandwich beam (a) Cylindrical bar strut of 1.5 mm diameter and 10 mm spacing; (b) Carbon fiber strut imbedded in core; (c) Rectangle shape strut inserted in core (d) Sandwich with added aerogel layers

Table 1 Dimensions of sandwich beam

Name	Length *X*	Length *Y*	Length *Z*	Volume mm^2	Mass Kg	Nodes	Element	Skin mm
Length	150	80	9	60000	0.471	12300	8880	1

2.2 Loads and Boundary Conditions

Axial load case was considered in sandwich buckling while point load was applied in bending tests of sandwich. However, for the buckling of sandwich beam structures, simply supported (pinned at both ends) conditions were used which could only move laterally, and in bending tests, sandwich structures were treated as cantilever Beams (fixed at one end and point load on the other end), as shown in Fig. 2(a). In buckling, no displacement along z-direction, completely fixed on one side and moving on the other side along the direction of applied force, in this case x-direction, as shown in Fig. 2(b). Fig. 2(c) depicts thermal boundary conditions (high temperature applied on top skin and room temperature set at bottom skin). Finally, Fig. 2(d) shows thermal boundary conditions for the temperature that could buckle the sandwich beam.

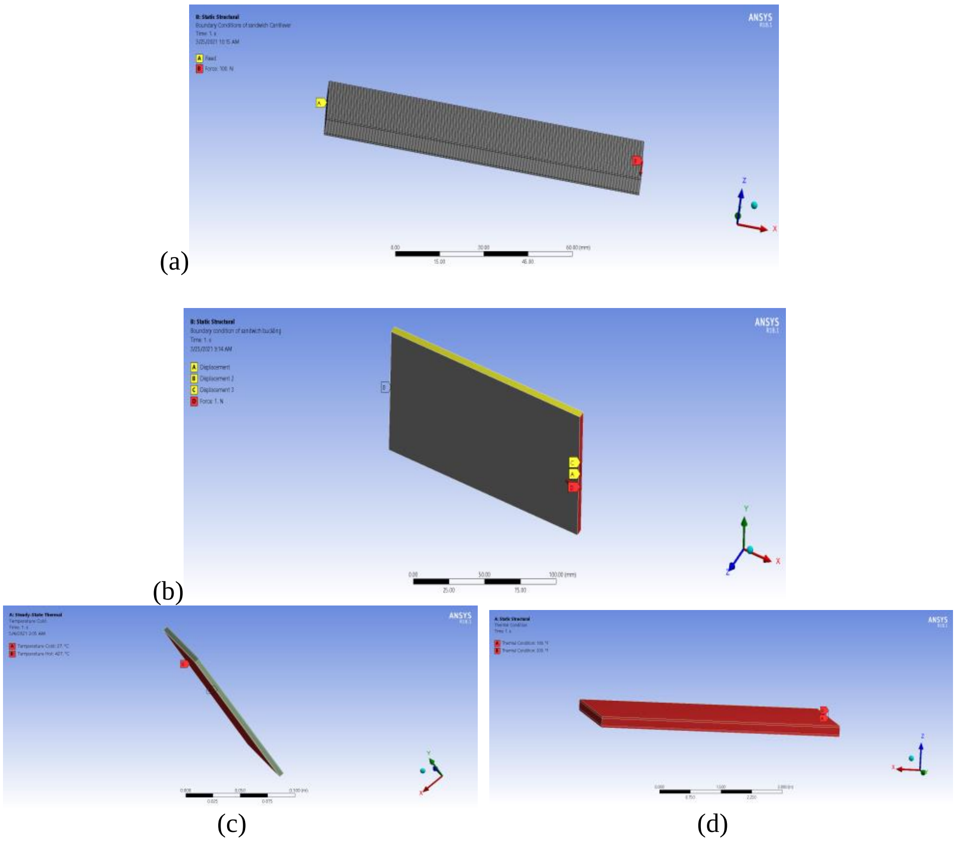

Fig. 2 Boundary conditions (a) cantilever for bending analysis; (b) simply supported, moving along horizontal direction; (c) steady-state temperature boundary condition (higher temperature applied on top skin); (d) Thermal expansion of sandwich beam

2.3 Material Properties

There has been extensive research on silica aerogels recently. As the lightest processed solid material on the planet, aerogels have the highest empty volume fraction in their structure. They are made by super critically drying silica gels, which was also the first inorganic aerogel to be developed by Patil et al. [115]. In this analysis aerogel was used for the reduction of heat flux, thermal strain and expansion.

Sandwich beam materials consist of carbon fiber-polyimide for skins and carbon foam as core. Ogasawara et al. [116] used the same structure to develop an effective heat-resistant sandwich panel. Table 2 summarizes the depicted material properties, carbon fiber-polyimide was used as face sheet and carbon foam was used as the core to analyze flexural strength in cantilever beam conditions and investigate strength along the axis (buckling). Furthermore, the sandwich beam with the same material was subjected to thermal loads and the results with and without aerogel were evaluated.

Table 2 Material properties of sandwich beams

Material	Young's Modulus *E* (MPa)	Poisson's Ratio *ν*	Shear Modulus *G* (MPa)	Density *ρ* (Kg/m^3)	Thermal conductivity (W/m°C)
Carbon fiber-polyimide	70000	0.36	25735	1410	2.16
Carbon foam	123.79	0.33	46538	2267	0.11
Silica Aerogel	5	0.2	20833	105	0.016

3. FEM ANALYSIS

ANSYS software was applied to perform numerical analysis on sandwich beams with carbon foam core. A linear buckling model was used in finite element analyses. The conceptual buckling strength of an ideal elastic structure was calculated using linear buckling (also known as eigenvalue buckling) and nonlinear analyses to investigate buckling temperature of sandwich beam. However, in contrast to linear solutions, non-linear solutions were also used in experiments to achieve the most precise results. Thereby, this method gave closer buckling estimation. Hence, critical buckling load (stress) and factors that optimize the sandwich structure were investigated and heat flow rate across sandwich layers was observed. All sandwich beam layers were modelled using solid model and was meshed using eight node solid elements SOLID186 (the total statistics of 8880 elements and 12300 nodes).

The details of the sandwich structure were b = 80 mm, L = 150 mm, t_f = 1 mm, t_c = 4 mm, E_f = 70000 MPa, P = 100 N, and E_c = 5 MPa. The faces of sandwich beam were made of carbon fiber-polyimide and its core was made of carbon foam. Tables 3, 4 and 5 show FEM results and analytical calculations.

Table3 Bending of cantilever sandwich beam structure

	Deformation (mm)
FEM	2.14
Analytical	2.17

Table 4 Buckling of sandwich beam structure

	Critical buckling load (N)
FEM	31097
Analytical	3167.1

Table 5 Heat flow rate of sandwich beam structure

	Heat flux (W/m^2)
FEM	2090.85
Analytical	2091.00

3.1 Global buckling of sandwich column

When studying sandwich systems, it is generally thought that the core only supports shear and that skins carry tensile and compressive loads under flexure [117]. The contributions of core and skin to flexural and shear stiffness were considered in the sandwich beams examined in this analysis.

Two modes of elastic buckling are possible: Euler buckling mode with sandwich column bending and a core shear mode. The shear deformation of core was taken into account in a more precise approach [118,119]. Fig. 3 shows the schematic model of buckling setup to find out plane displacement on sandwich beam.

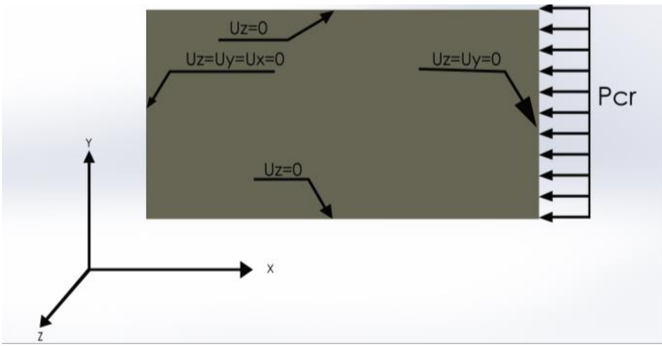

Fig. 3 Schematic model of buckling setup

For case of a strut with built-in ends (which are constrained against rotation), the Euler buckling load *PE* is:

$$PE = \frac{4\pi^2 (EI)_{eq}}{l^2} \tag{1}$$

The equivalent flexural stiffness EI_{eq} of the sandwich beams was calculated by Eq. (2).

$$EI_{eq} = \frac{bt^3}{6} E_f + \frac{btd^2}{2} E_f + \frac{bc^3}{12} E_c \tag{2}$$

where E_f and E_c are the Young's moduli of face sheet and core materials, respectively, *b* is the width of sandwich column, *t* is the thickness of face sheet, and *c* is the thickness of core. $d \equiv t + c$ is the distance between the mid-planes of face sheets.
The core shear buckling load *Ps* was set by the shear stiffness of core.

$$Ps = (AG)eq \tag{3}$$

where the corresponding shear rigidity of core (*AG*)*eq* is:

$$(AG)eq \approx bcGc \tag{4}$$

where $PS \approx AG_{eq}$, A = (*h* + *H*)2/*h*, $G_c = E_c/(1 + 2vc)$, G_c is the shear modulus of the core and *bc* the cross-sectional area of the core.
However, at transformation values of strut slenderness ratio, these buckling modes interacted to produce a combined collapse load (P_{cr}) where:

$$Pcr = PE + Ps \tag{5}$$

3.2 Heat transfer equations

Local heat flux for one-dimensional steady-state heat transfer across a sandwich, according to the Fourier heat transfer law, could be written as:

$$q = -k\Delta T = -k\frac{dT}{dx} \tag{6}$$

where q is local heat flux density (W/m^2), K is material thermal conductivity ($W/m*k$), $\Delta T = \frac{dT}{dx}$ is temperature gradient (K/m).

3.3 Thermal resistance

Thermal resistance is a thermal property and a measurement of how well a material resists a heat flow.

$$Q_{wall} = -kA\frac{T_2 - T_1}{L} = -\frac{T_2 - T_1}{R_{thcond}} \tag{7}$$

$$Rskin = \frac{t}{K_s A} \tag{8}$$

$$Rcore = \frac{t}{K_c A} \tag{9}$$

$$R_{thcond} = 2(\ Rskin) + R\ core \tag{10}$$

where ΔT is the amount of heat transited through sandwich beam $(T_2 - T_1)$, R_{thcond} represents thermal conductive resistance, L is length, t is thickness, A is area, K_s is the thermal conductivity of skin and K_c is the thermal conductivity of core. Hence, in this analysis, temperature was applied on the bottom and top face sheets of the sandwich beam. Fig. 4 depicts the schematic model of conductive heat distribution on sandwich beam and showed that high heat was transferred from the top skin, distributed through core and down to bottom skin.

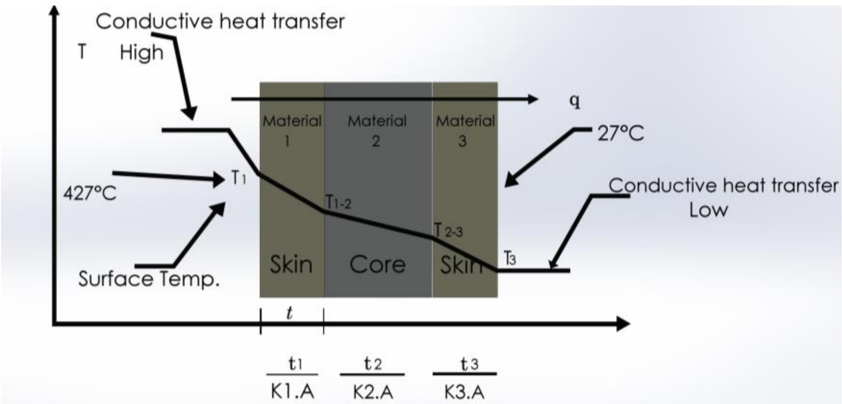

Fig. 4 Schematic model of conductive heat distribution on sandwich beam.

4. RESULTS AND OBSERVATION

4.1 Deformation of Sandwich

Considering the deformation of sandwich beam shape due to applied forces and change in temperature, in order to investigate total deformation and the state of stresses. This analysis considered the buckling of sandwich beam due to applied forces and elevated temperature, bending of sandwich due to applied loads and heat flow rate across the sandwich beam.

4.2 Buckling Analysis

In order to determine the failure mode in which relatively large deflections occurred on sandwich beam, buckling analysis was carried out to investigate what load and temperature level caused buckling and elastic instability on sandwich structures. Moreover, sandwich deformation nature was investigated by determining the temperature that buckled the sandwich, according to the material properties used for sandwich beam. Furthermore, simulation was carried out on two sandwich beams, one with carbon fiber strut in the core and the other without carbon fiber strut. Fig. 5 depicts the buckling nature of the sandwich beam without carbon fiber strut. Furthermore, the same procedure was applied to observe the buckling nature of the sandwich with imbedded strut as shown in Fig. 6. In this case, temperature was not added in static structural analyzer and the results showed improvement in buckling load for the sandwich with carbon fiber circular strut, as shown in Table 6.

Table 6 Buckling load

Sandwich type	Buckling Load (N)
Sandwich with circular strut imbedded in core	34413
Sandwich without circular strut	31017

(a)
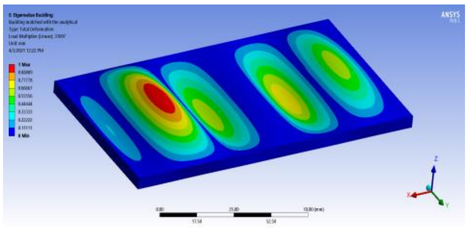

(b)
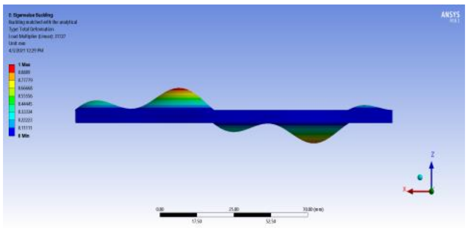

Fig. 5 Buckling of sandwich under axial compression (a) isometric view; (b) side view

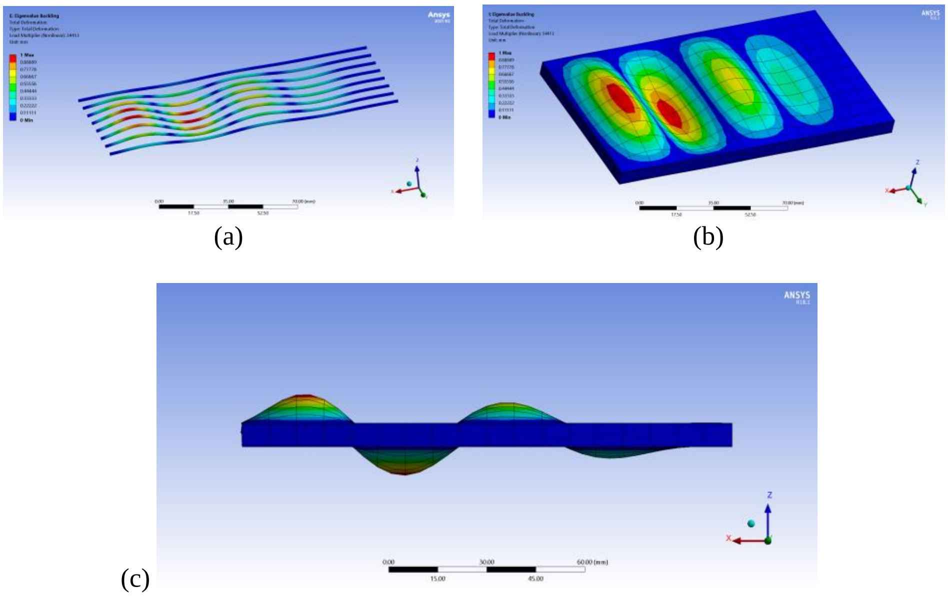

Fig. 6 (a) Cylindrical carbon fiber imbedded in the core (diameter of 1.5 mm)
(b) Buckling of sandwich under axial compression (isometric view);
(c) Buckling of sandwich under axial compression (side view**)**

4.3 Buckling Analysis with Thermal Expansion

Nonlinear buckling was simulated through a static structural analysis in ANSYS. Temperature was raised and sandwich buckling was observed. To begin with, analytical settings in structural run were set and large deflection was turned on. In addition, boundary was assigned, x movements on both sides were constraint to confine the sandwich beam during thermal expansion in order to observe compressive stresses along x-direction. Furthermore, sandwich vertex were prevented from moving along z-direction and finally the left and right sandwich beam edges were restricted from moving vertically. In general, sandwich beam could not expand thermally along x-direction, and expanded only along y and z directions due to the constraints; it was not free to translate and rotate globally.

4.3.1 Load

Environment temperature of 70 °F was assigned to sandwich beam in static structural analysis and the thermal condition of sandwich beam was 100 °F. Hence, in this analysis, there was a 30 °F temperature increase that caused thermal expansion. Therefore, temperature that caused state of stresses on the sandwich beam were noted. Hence, Fig. 7(a) shows the first mode shape, the sandwich beam were quizzed due to thermal load and not allowed to move globally which caused it to buckle in the middle. However, as there was 30 °F difference which was the only load on sandwich beam and was multiplied by load multiplier of the first mode in eigenvalue buckling module and summed with 70°F environmental temperature assigned early which resulted to the buckling temperature of

140.47°F. The same analysis was repeated for sandwich structures with aerogel layers, in order to investigate effect of aerogel layers and the corresponding bucking temperature. Fig. 7 shows the 3 modes of sandwich beam without silica aerogel. Moreover, the first mode was considered the most. Fig. 8 shows aerogel position in the sandwich beam and first 2 mode shapes of sandwich beam with silica aerogel material. Table 7 summarizes the temperature causing buckling on both sandwich beams with and without aerogel layers. There was 6% increase in temperature that could buckle the sandwich beam when silica aerogel was used.

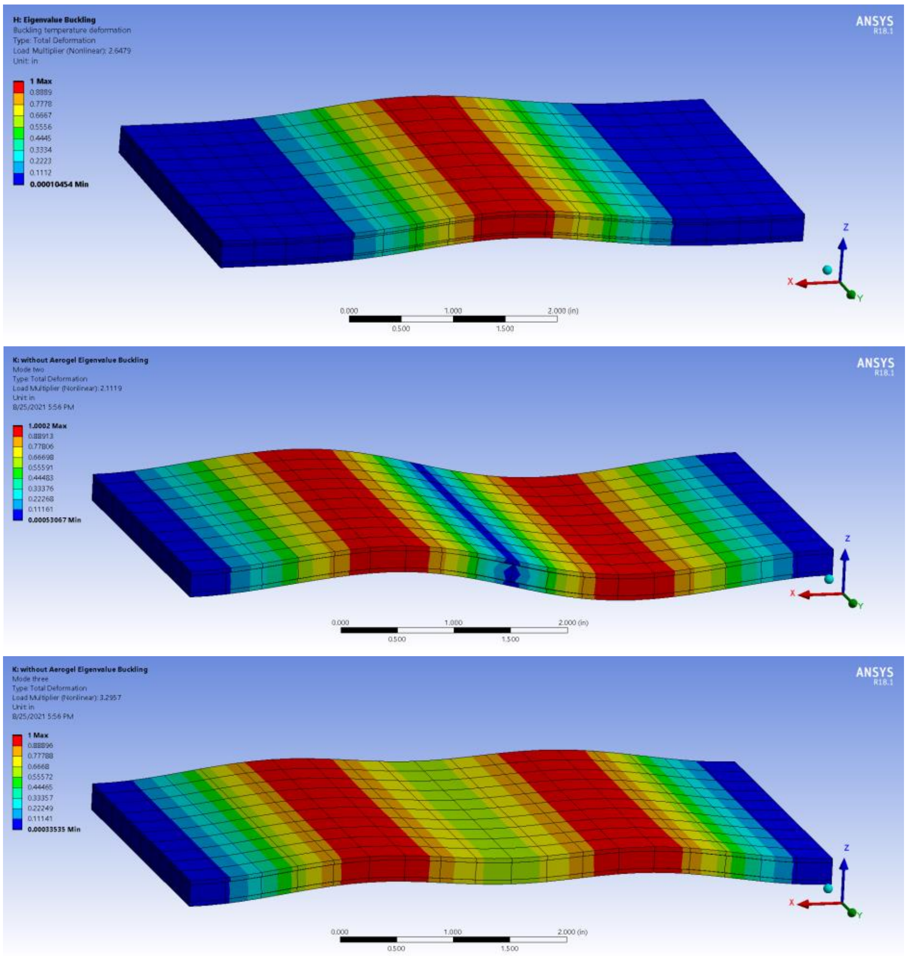

(a) (b) (c)

Fig. 7 Mode shapes of sandwich beam without silica aerogel (a) Mode 1; (b) Mode 2; and (c) Mode 3

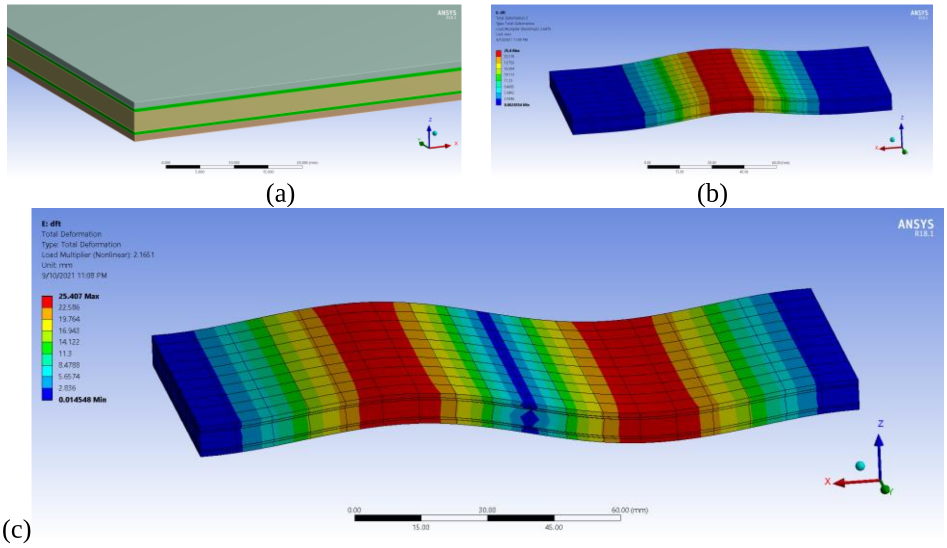

Fig. 8 Mode shapes of sandwich beam with silica aerogel (a) Sandwich beam with silica aerogel addition; (b) Mode 1; (c) Mode 2

Table 7 Buckling Temperature

Sandwich type	Buckling Temperature (°F)
Sandwich with silica aerogel	149.44
Sandwich without silica aerogel	140.47

4.4 Bending of Sandwich

To evaluate both the ductility and soundness of a material, sandwich structure was treated as cantilever beam with one end fixed and point load of 100 N at the other end. Hence, deformation occurred and stress was observed and analysis was carried out on the three components of sandwich, top skin, core and bottom skin. Therefore, it was observed that the maximum deformation and stress were on the top face sheet as depicted in Fig. 9(a). Also, Fig. 9(b) shows deformation on sandwich core while Fig. 9(c) depicts the bottom skin deformation where both the stress and deformation are at minimum. Hence, with the same boundary and loading conditions, in order to improve the flexural stiffness, rectangular shaped carbon fiber was added to the core. Moreover, Fig. 10(a) and 10(b) depicts the detailed and overlay views of rectangular carbon fiber on sandwich core, respectively. Fig. 10(c) shows the stresses absorbed by carbon fiber rectangular strut. In addition, Fig. 11 illustrates the total deformation of the sandwich beam under different applied forces. As a results of that, the sandwich beam with imbedded rectangular shaped carbon fiber has less deformation when compared to sandwich beam without carbon fiber. Hence, for sandwich beam deformation, Fig. 12 shows the effect of core thickness on deformation. Core thickness was increased by 0.2 mm which significantly reduced deformation. Therefore, there was a good correlation between core thickness and deformation; as core thickness was increased, deformation was decreased.

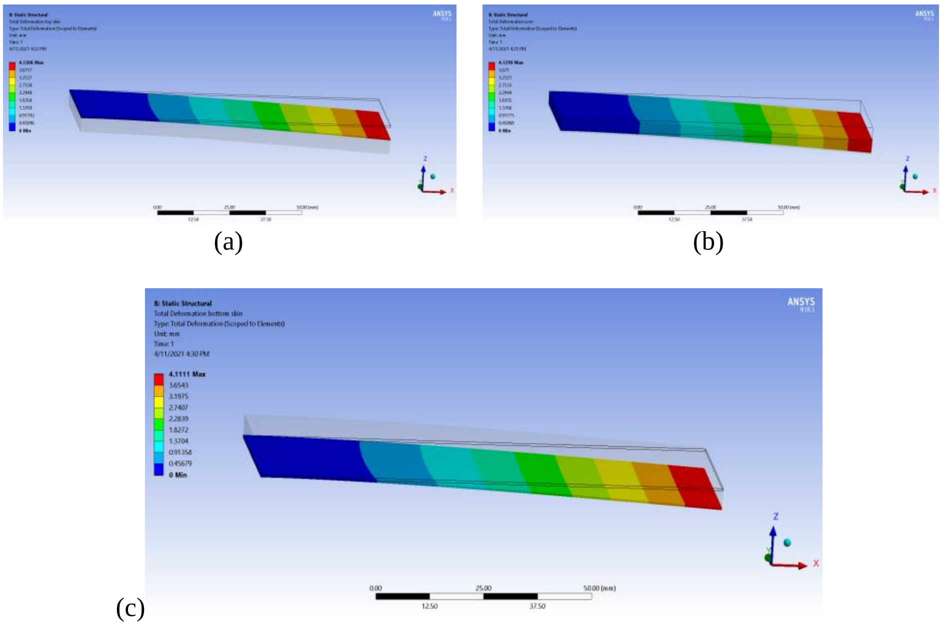

Fig. 9 Deformation of sandwich (a) Deformation at top skin; (b) Deformation at core; (c) Deformation at bottom skin

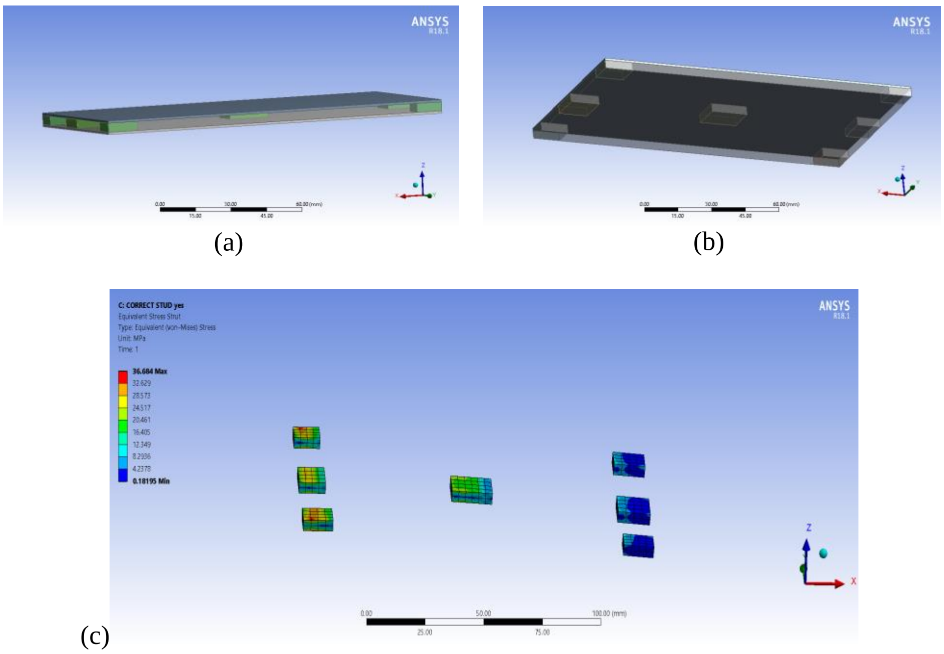

Fig. 10 Deformation of sandwich with reinforced carbon fiber (a) sandwich view 1; (b) Sandwich view 2; (c) Stresses acting on rectangular carbon fiber

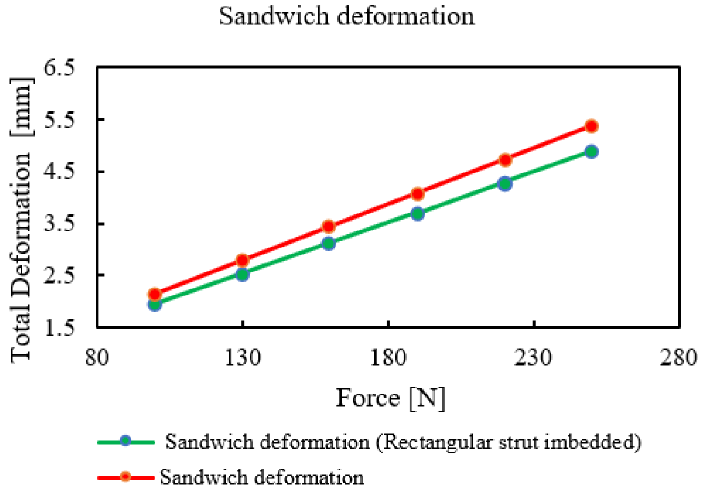

Fig. 11 Applied force vs. total deformation of sandwich beam

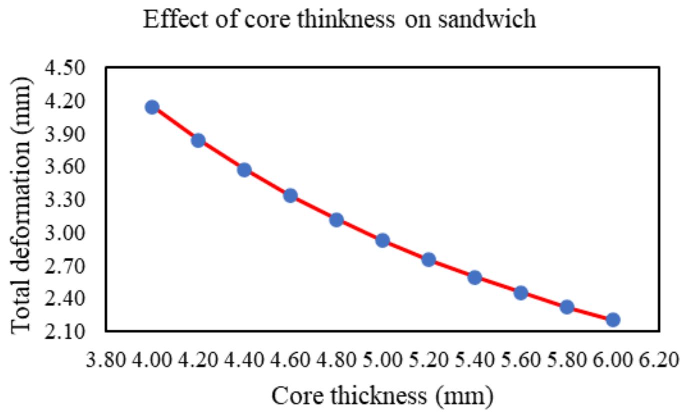

Fig. 12 Core thickness (mm) vs. total deformation (mm)

4.5 Conduction Thermal Analysis of Sandwich Beam and Stresses

In order to investigate heat transfer, Sandwich structure was made of more than one material, thermal loads and effective factors of the sandwich were observed. Moreover, a change in temperature produced thermal strains which could cause sandwich deformation. The analysis was conducted under steady state thermal module in ANSYS and the solution was imported into static structural module for the observation of thermal strain and mechanical stress. Temperature of 427 °C was applied to top skin and 22 °C to bottom skin. It was assumed that the sandwich beam was used as cover structure which emitted high temperature. The effects of temperature increase from bottom face sheet to top face sheet (T = 22°C to 427 °C) for the sandwich of carbon fiber-polyimide face skin and carbon foam core are shown in Fig. 13. At high temperatures, thermal stress was increased from minimum to maximum causing expansion on the top face, as shown in Fig. 14. Hence, there was some deformation in bottom skin (contraction), as shown in Fig. 15. Similarly, silica aerogel with the thickness of 0.5 mm was added as shown in Fig. 16. Fig. 17 shows the corresponding thermal strain nature of the sandwich beam. As a result of considering the heat conduction of the sandwich, based on review [116], carbon fiber-polyimide and carbon foam materials were used. Fig. 18(a) shows the deformation of aerogel layer on the hot side while Fig. 18(b) depicts the thermal deformation of aerogel material only bonded between top skin and core. In addition, Fig. 18(c) shows thermal strain on the bottom skin of the sandwich beam. It was found that thermal strain was minimal on the sandwich beam due to the addition of silica aerogel layers and the top skin did not deform so much as compared when silica aerogel was not added. In general, it was observed that there was significant decrease in heat flux when silica aerogel was added, as depicted in Fig. 19. Sandwich beam was subjected to high temperature ranging from 100 °C to 430 °C and the corresponding heat flux was recorded for sandwich beams with and without aerogel material. The results showed that the sandwich beam with silica aerogel had significant heat transfer resistance, as shown in Fig. 19. Similarly, simulation was repeated, in this case thermal deformation was considered and results showed that sandwich beam with aerogel layers had good thermal strain resistance, as depicted in Fig. 20. However, thermal deformation was decreased by 17.6% when silica aerogel was added as layer. In this analysis, 0.5 mm aerogel layer improved thermal strain by about 17.6%.

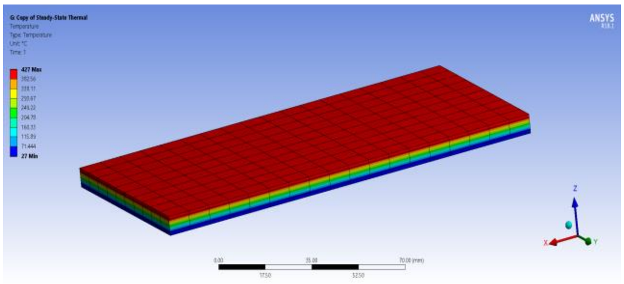

Fig. 13 Temperature distribution across the top and bottom skins, temperature increasing from T = 27 °C to 427 °C

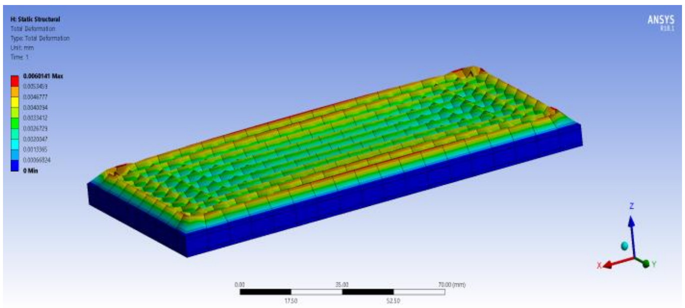

Fig. 14 Sandwich structure showing deformation on the top face at 427 °C (carbon foam core used)

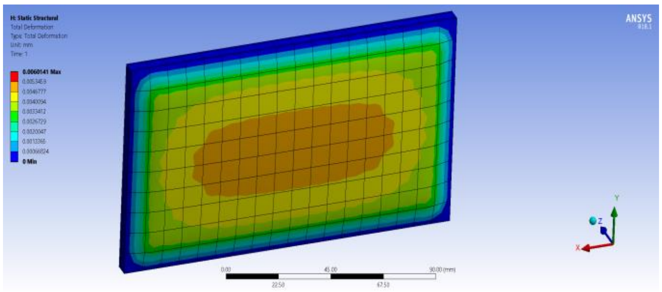

Fig. 15 Sandwich structure showing deformation on the bottom face at 427 °C

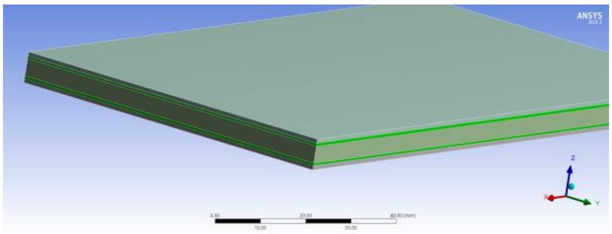

Fig. 16 Sandwich structure with silica aerogel layer

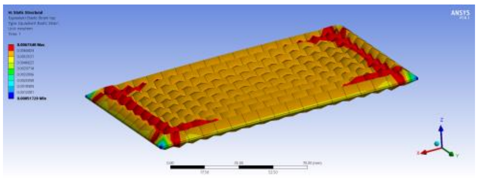

(a)

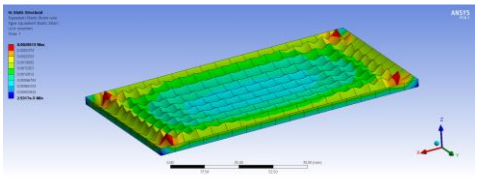

(b)

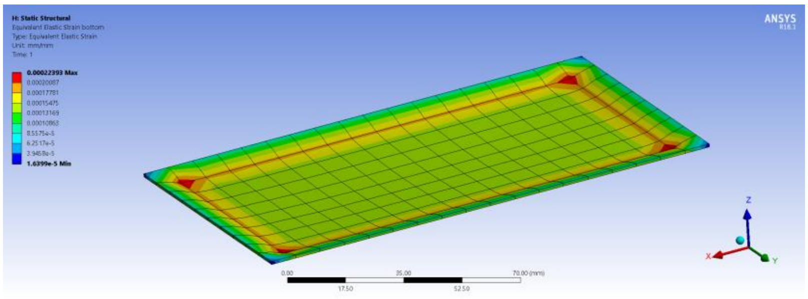

(c)

Fig. 17 Thermal strain on (a) top skin; (b) core; and (c) bottom skin (Scale 0.5x auto)

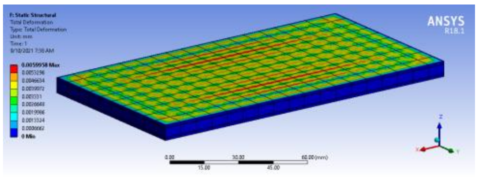

(a)

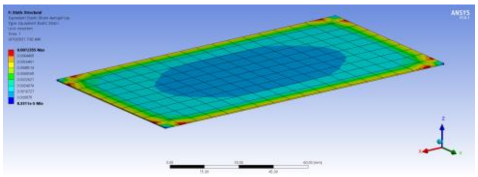

(b)

(c)

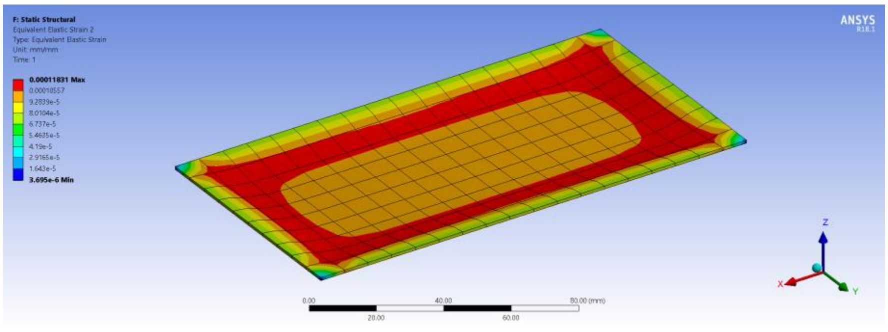

Fig. 18 Sandwich with aerogel layer. (a) Sandwich structure showing deformation on the top face at 427 °C (carbon foam core and aerogel layer used); (b) Thermal strain on top aerogel layer; (c) thermal strain on bottom skin

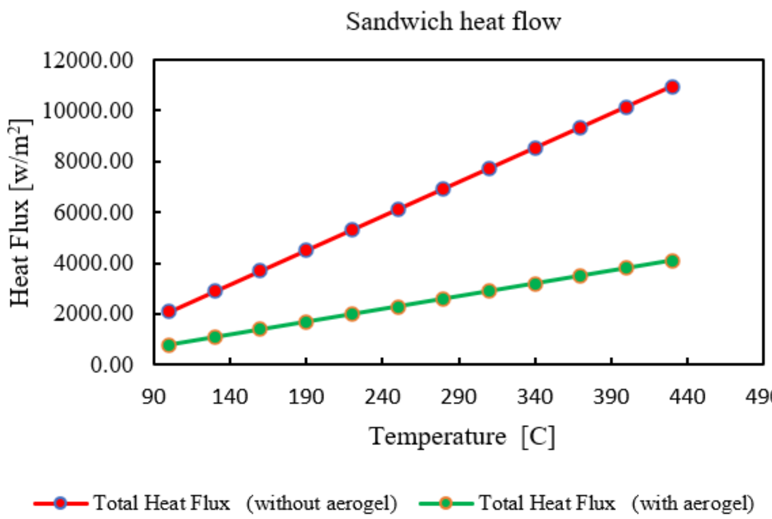

Fig. 19 Change in temperature Vs. heat flux of sandwich

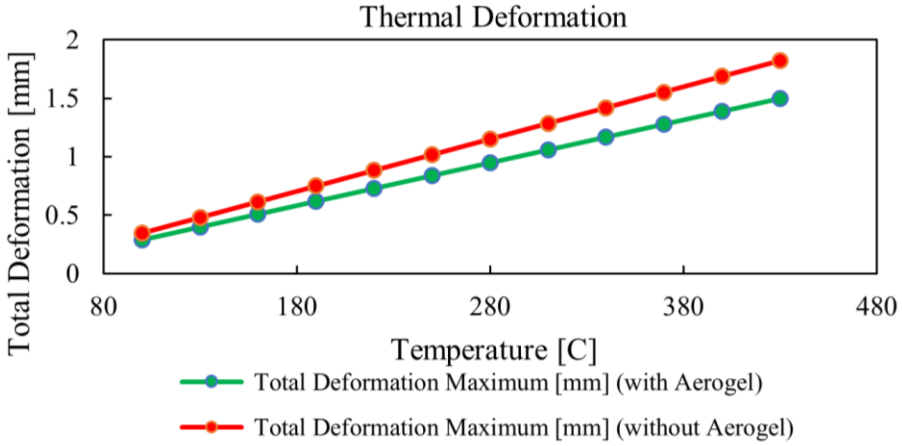

Fig. 20 Change in temperature Vs. thermal deformation of sandwich beam

4.6. Analysis and Comparison

The experimental approaches developed by Goswami [120] were simulated and modified. Goswami used aramid sheet for skin and aramid hexagonal honeycomb core, filled with silica aerogel. The setup was separated into two parts: heating system (part A) where the heater was installed on the top face sheet of the sandwich with thermocouple arrangements while only the thermocouple was installed on the bottom face sheet (part B). Temperature increase stopped at 350 ºC because the manufacturer specified that the flash point of silica aerogel has to be 395 ºC.

Fig. 21 shows heat flux on honeycomb sandwich panel in three cases;

1) Honeycomb filled with silica aerogel.
2) Honeycomb with silica aerogel as auxiliary face sheet.
3) Honeycomb without silica aerogel.

The results showed that the honeycomb with silica aerogel as an auxiliary face sheet had lower heat flux, thereby providing good heat insulation in the honeycomb sandwich beam.

In ANSYS workbench, a thermal analysis experiment was simulated and the results were validated. Moreover, the honeycomb filled with silica aerogel as shown in Fig. 22(a) has higher temperature difference (The heat will take longer to transfer from one side to the other) than the one without silica aerogel as depicted in Fig. 22(b). Furthermore, the methods used by Goswami in the experiment was by no means the most effective approach towards providing heat insulation in the honeycomb sandwich as there was much heat flow in honeycomb cell walls, as shown in Fig. 22(c). In general, silica aerogel was used as an auxiliary face sheet before the honeycomb hexagonal core as depicted in Fig. 22(d). Therefore, heat flow was minimal and evenly distributed through the honeycomb core, as shown in Fig. 22(e).

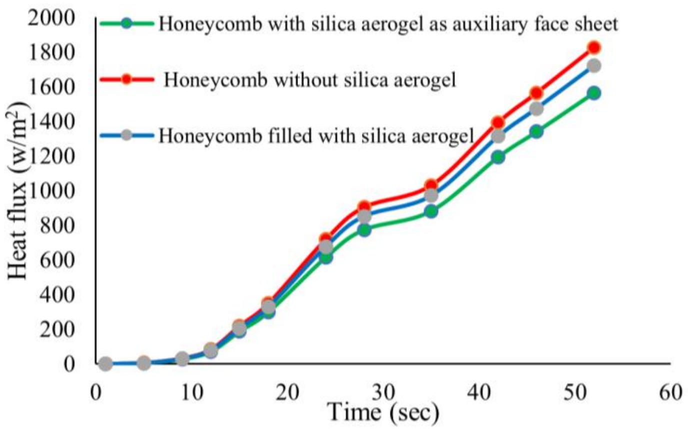

Fig. 21 Time vs. heat flux of sandwich panel

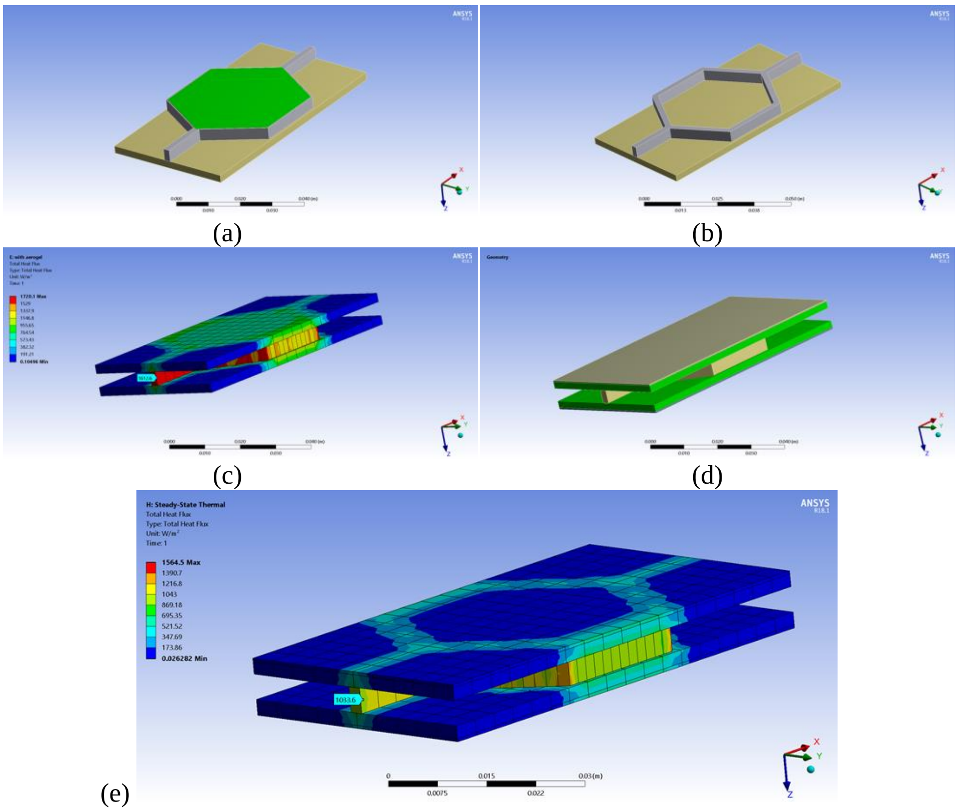

Fig. 22 Honeycomb sandwich panel: (a) Honeycomb filled with silica aerogel; (b) Honeycomb without silica aerogel; (c) Heat flow in honeycomb cell walls on honeycomb filled with silica aerogel; (d) Silica aerogel as auxiliary face sheet; (e) Reduced heat flow on core cell walls (silica aerogel as auxiliary face sheet)

5. CONCLUSION

The findings of a detailed study and simulation were shown and plotted and important observations were recorded. Thermal stresses and buckling temperature were improved by the addition of silica aerogel material. Steady state condition of the sandwich beam was investigated in commercial software ANSYS and the temperature induced stress and the nature of thermal expansion-induced deformation were noted. Hence, the parameters affecting thermal strain and heat flow were mechanical properties and the most significant one was thermal conductivity, as we considered the heat conduction of the sandwich beam (heat flux). In addition, experimental approach was simulated and modified. Filling hexagonal honeycomb cells with silica aerogel was not the most effective way of heat reduction in the sandwich but it could be used as an auxiliary face sheet. Moreover, carbon foam with lower thermal conductivity was further improved by the addition of silica aerogel layer which was the lightest and hence had the mass of 1.22 g and extreme heat flow resistance. As a result of flexural strength, the sandwich was imbedded with rectangular shaped and cylindrical bar carbon fiber strut in the core, thereby improving stiffness and buckling load. Addition of carbon fiber strut was effective in maintaining flexural strength while keeping the core thickness minimal. In general, silica aerogel is a good thermal insulator and extremely light material. Furthermore, in aerospace and electronics industries, the application of fiberglass insulation should be minimized and replaced with a small amount of aerogel.

REFERENCE

1. Darzi, S., Karampour, H., Bailleres, H., Gilbert, B.P., Fernando, D., 2020, *Load bearing sandwich timber walls with plywood faces and bamboo core*, Structures, 27, pp. 2437–2450.
2. Gay, D., Suong, V., 2003, *HOA a Stephen W. TSAI*, Composite materials: design and applications, doi: 10.1201/9781420031683
3. Ashby, M.F., Cebon, D., 1993, *Materials selection in mechanical design*, Le Journal de Physique IV, 3(C7), pp. C7-1.
4. Gibson, L.J., 2003, *Cellular solids*, Mrs Bulletin, 28(4), pp. 270–274.
5. Douville, M.A., Le Grognec, P., 2013, *Exact analytical solutions for the local and global buckling of sandwich beam-columns under various loadings*, International Journal of Solids and Structures, 50(16–17), pp. 2597–2609.
6. Zhang, F., Liu, W., Ling, Z., Fang, H., Jin, D., 2018, *Mechanical performance of GFRP-profiled steel sheeting composite sandwich beams in four-point bending*, Composite Structures, 206, pp. 921–932.
7. Sohel, K.M.A., Richard Liew, J.Y., 2011, *Steel–Concrete–Steel sandwich slabs with lightweight core — Static performance*, Engineering Structures, 33(3), pp. 981–992.
8. Reyes, G., 2008, *Static and low velocity impact behavior of composite sandwich panels with an aluminum foam core*, Journal of Composite Materials, 42(16), pp. 1659–1670.
9. Mamalis, A.G., Spentzas, K.N., Manolakos, D.E., Ioannidis, M.B., Papapostolou, D.P., 2008, *Experimental investigation of the collapse modes and the main crushing characteristics of composite sandwich panels subjected to flexural loading*, International Journal of Crashworthiness, 13(4), pp. 349–362.
10. Crupi, V., Epasto, G., Guglielmino, E., 2012, *Collapse modes in aluminium honeycomb sandwich panels under bending and impact loading*, International Journal of Impact Engineering, 43, pp. 6–15.
11. Correia, J.R., Garrido, M., Gonilha, J.A., Branco, F.A., Reis, L.G., 2012, *GFRP sandwich panels with PU foam and PP honeycomb cores for civil engineering structural applications: Effects of introducing strengthening ribs*, International journal of structural integrity, 3(2) pp. 127–147.
12. Qin, Y., Kang, R., Sun, J., Wang, Y., Zhu, X., Dong, Z., 2022, *A fast self-calibration method of line laser sensors for on-machine measurement of honeycomb cores*, Optics and Lasers in Engineering, 152, 106981.

13. Davalos, J.F., Qiao, P., Frank Xu, X., Robinson, J., Barth, K.E., 2001, *Modeling and characterization of fiber-reinforced plastic honeycomb sandwich panels for highway bridge applications*, Composite Structures, 52(3), pp. 441–452.
14. Camata, G., Shing, P.B., 2010, *Static and fatigue load performance of a gfrp honeycomb bridge deck*, Composites Part B: Engineering, 41(4), pp. 299–307.
15. Sorohan, Ş., Sandu, M., Sandu, A., Constantinescu, D.M., 2016, *Finite Element Models Used to Determine the Equivalent In-plane Properties of Honeycombs*, Materials Today: Proceedings, 3(4), pp. 1161–1166.
16. Kalaprasad, G., Pradeep, P., Mathew, G., Pavithran, C., Thomas, S., 2000, *Thermal conductivity and thermal diffusivity analyses of low-density polyethylene composites reinforced with sisal, glass and intimately mixed sisal/glass fibres*, Composites Science and Technology, 60(16), pp. 2967–2977.
17. Sahraoui, S., Mariez, E., Etchessahar, M., 2000, *Mechanical testing of polymeric foams at low frequency*, Polymer Testing, 20(1), pp. 93–96.
18. Quintana, J.M., Mower, T.M., 2017, *Thermomechanical behavior of sandwich panels with graphitic-foam cores*, Materials & Design, 135, pp. 411–422.
19. Subedi, N.K., Coyle, N.R., 2002, *Improving the strength of fully composite steel-concrete-steel beam elements by increased surface roughness—an experimental study*, Engineering Structures, 24(10), pp. 1349–1355.
20. Subedi, N.K., 2003, *Double skin steel/concrete composite beam elements: experimental testing*, Structural Engineer, 81(21), pp. 30–35.
21. Daniel, I.M., Abot, J.L., 2000, *Fabrication, testing and analysis of composite sandwich beams*, Composites Science and Technology, 60(12–13), pp. 2455–2463.
22. Vaikhanski, L., Nutt, S.R., 2003, *Fiber-reinforced composite foam from expandable PVC microspheres*, Composites Part A: Applied Science and Manufacturing, 34(12), pp. 1245–1253.
23. Hadi, B.K., Matthews, F.L., 2000, *Development of Benson–Mayers theory on the wrinkling of anisotropic sandwich panels*, Composite Structures, 49(4), pp. 425–434.
24. Gdoutos, E.E., Daniel, I.M., Wang, K.-A., 2003, *Compression facing wrinkling of composite sandwich structures*, Mechanics of Materials, 35(3), pp. 511–522.
25. Jiang, W., Liu, Y., 2017, *Indentation of rigidly supported sandwich beams with core gradation*, International Journal of Mechanical Sciences, 134, pp. 182–188.
26. Li, Z., Chen, X., Jiang, B., Lu, F., 2016, *Local indentation of aluminum foam core sandwich beams at elevated temperatures*, Composite Structures, 145, pp. 142–148.
27. Ha, G.X., Marinkovic, D., Zehn, M.W., 2019, *Parametric investigations of mechanical properties of nap-core sandwich composites*, Composites Part B: Engineering, 161, pp. 427–438.
28. McCormack, T.M., Miller, R., Kesler, O., Gibson, L.J., 2001, *Failure of sandwich beams with metallic foam cores*, International Journal of Solids and Structures, 38(28), pp. 4901–4920.
29. Ha, G.X., Zehn, M.W., Marinkovic, D., Fragassa, C., 2019, *Dealing with Nap-Core Sandwich Composites: How to Predict the Effect of Symmetry*, Materials, 12(6), 874.
30. Fu, J.W., Akbarzadeh, A.H., Chen, Z.T., Qian, L.F., Pasini, D., 2016, *Non-Fourier heat conduction in a sandwich panel with a cracked foam core*, International Journal of Thermal Sciences, 102, pp. 263–273.
31. Mehar, K., Kumar Panda, S., 2018, *Thermal free vibration behavior of FG-CNT reinforced sandwich curved panel using finite element method*, Polymer Composites, 39(8), pp. 2751–2764.
32. Sun, S., Sheng, Y., Feng, S., Jian Lu, T., 2021, *Heat transfer efficiency of hierarchical corrugated sandwich panels*, Composite Structures, 272, 114195.
33. Onyibo, E.C., Safaei, B., 2022, *Application of finite element analysis to honeycomb sandwich structures: a review*, Reports in Mechanical Engineering, 3(1), pp. 283–300.
34. Su, B., Chen, J., Hao, J., Fan, X., Han, X., 2020, *Thermal insulation performance of GFRP squared tube reinforced sandwich panel*, Energy and Buildings, 211, 109790.
35. Moradi-Dastjerdi, R., Behdinan, K., 2021, *Temperature effect on free vibration response of a smart multifunctional sandwich plate*, Journal of Sandwich Structures and Materials, 23(6), pp. 2399–2421.
36. Zhang, L., Zhang, F., Qin, Z., Han, Q., Wang, T., Chu, F., 2022, *Piezoelectric energy harvester for rolling bearings with capability of self-powered condition monitoring*, Energy, 238, 121770.
37. Zhao, W., Liu, Z., Yu, G., Wu, L., 2021, *A new multifunctional carbon fiber honeycomb sandwich structure with excellent mechanical and thermal performances*, Composite Structures, 274, 114306.
38. Safaei, B., Naseradinmousavi, P., Rahmani, A., 2016, *Development of an accurate molecular mechanics model for buckling behavior of multi-walled carbon nanotubes under axial compression*, Journal of Molecular Graphics and Modelling, 65, pp. 43–60.
39. Chen, Y., Zhang, L., He, C., He, R., Xu, B., Li, Y., 2021, *Thermal insulation performance and heat transfer mechanism of C/SiC corrugated lattice core sandwich panel*, Aerospace Science and Technology, 111, 106539.

40. Safaei, B., Moradi-Dastjerdi, R., Behdinan, K., Qin, Z., Chu, F., 2019, *Thermoelastic behavior of sandwich plates with porous polymeric core and CNT clusters/polymer nanocomposite layers*, Composite Structures, 226, 111209.
41. Asmael, M., Safaei, B., Zeeshan, Q., Zargar, O., Nuhu, A.A., 2021, *Ultrasonic machining of carbon fiber–reinforced plastic composites: a review*, International Journal of Advanced Manufacturing Technology, 113(11–12), pp. 3079-3120.
42. Safaei, B., 2021, *Frequency-dependent damped vibrations of multifunctional foam plates sandwiched and integrated by composite faces*, European Physical Journal Plus, 136(6), 646
43. Liu, Y., Qin, Z., Chu, F., 2021, *Nonlinear forced vibrations of FGM sandwich cylindrical shells with porosities on an elastic substrate*, Nonlinear Dynamics, 104(2), pp. 1007–1021.
44. Hadji, L., Avcar, M., 2021, *Free Vibration Analysis of FG Porous Sandwich Plates under Various Boundary Conditions*, Journal of Applied and Computational Mechanics, 7(2), pp. 505–519.
45. Li, H., Lv, H., Sun, H., Qin, Z., Xiong, J., Han, Q., Liu, J., Wang, X., 2021, *Nonlinear vibrations of fiber-reinforced composite cylindrical shells with bolt loosening boundary conditions*, Journal of Sound and Vibration, 496, 115935.
46. Liu, Y., Qin, Z., Chu, F., 2021, *Nonlinear forced vibrations of functionally graded piezoelectric cylindrical shells under electric-thermo-mechanical loads*, International Journal of Mechanical Sciences, 201, 106474.
47. Sahmani, S., Aghdam, M.M., 2018, *Nonlinear primary resonance of micro/nano-beams made of nanoporous biomaterials incorporating nonlocality and strain gradient size dependency*, Results in Physics, 8, pp. 879–892.
48. Azizi, S., Safaei, B., Fattahi, A.M., Tekere, M., 2015, *Nonlinear vibrational analysis of nanobeams embedded in an elastic medium including surface stress effects*, Advances in Materials Science and Engineering, 2015, pp. 1-7
49. Li, H., Li, Z., Safaei, B., Rong, W., Wang, W., Qin, Z., Xiong, J., 2021, *Nonlinear vibration analysis of fiber metal laminated plates with multiple viscoelastic layers.* Thin-Walled Structures, 168, 108297
50. Li, Q., Xie, B., Sahmani, S., Safaei, B., 2020, *Surface stress effect on the nonlinear free vibrations of functionally graded composite nanoshells in the presence of modal interaction*, Journal of the Brazilian Society of Mechanical Sciences and Engineering, 42(5), pp. 1–18.
51. Sahmani, S., Fattahi, A.M., Ahmed, N.A., 2020, *Surface elastic shell model for nonlinear primary resonant dynamics of FG porous nanoshells incorporating modal interactions*, International Journal of Mechanical Sciences, 165, 105203.
52. Safaei, B., Fattahi, A.M., 2017, *Free vibrational response of single-layered graphene sheets embedded in an elastic matrix using different nonlocal plate models*, Mechanika, 23(5), pp. 678–687.
53. Yi, H., Sahmani, S., Safaei, B., 2020, *On size-dependent large-amplitude free oscillations of FGPM nanoshells incorporating vibrational mode interactions*, Archives of Civil and Mechanical Engineering, 20(2), pp. 1–23.
54. Xie, B., Sahmani, S., Safaei, B., Xu, B., 2021, *Nonlinear secondary resonance of FG porous silicon nanobeams under periodic hard excitations based on surface elasticity theory*, Engineering with Computers, 37(2), pp. 1611–1634.
55. Sahmani, S., Bahrami, M., Aghdam, M.M., Ansari, R., 2014, *Surface effects on the nonlinear forced vibration response of third-order shear deformable nanobeams*, Composite Structures, 118(1), pp. 149–158.
56. Yang, Z., Zhao, S., Yang, J., Lv, J., Liu, A., Fu, J., 2021, *In-plane and out-of-plane free vibrations of functionally graded composite arches with graphene reinforcements*, Mechanics of Advanced Materials and Structures, 28(19), pp. 2046–2056
57. Katariya, P. V., Panda, S.K., Mahapatra, T.R., 2018, *Bending and vibration analysis of skew sandwich plate*, Aircraft Engineering and Aerospace Technology, 90(6), pp. 885–895.
58. Liu, Y., Qin, Z., Chu, F., 2022, *Investigation of magneto-electro-thermo-mechanical loads on nonlinear forced vibrations of composite cylindrical shells*, Communications in Nonlinear Science and Numerical Simulation, 107, 106146.
59. Moradi-Dastjerdi, R., Behdinan, K., 2021, *Free vibration response of smart sandwich plates with porous CNT-reinforced and piezoelectric layers*, Applied Mathematical Modelling, 96, pp. 66–79.
60. Bažant, Z.P., Beghini, A., 2004, *Sandwich buckling formulas and applicability of standard computational algorithm for finite strain*, Composites Part B: Engineering, 35(6–8), pp. 573–581.
61. Wang, D., Abdalla, M.M., 2015, *Global and local buckling analysis of grid-stiffened composite panels*, Composite Structures, 119, pp. 767–776.
62. Hu, H., Belouettar, S., Potier-Ferry, M., Makradi, A., 2009, *A novel finite element for global and local buckling analysis of sandwich beams*, Composite Structures, 90(3), pp. 270–278.

63. Zhao, T., Yu, F., 2020, *Critical upheaval buckling forces of sandwich pipelines with variable stiffnesses of pipe material*, Ocean Engineering, 217, 107547.
64. Alhijazi, M., Safaei, B., Zeeshan, Q., Asmael, M., 2021, *Modeling and simulation of the elastic properties of natural fiber-reinforced thermosets*, Polymer Composites, 42(7), pp. 3508–3517.
65. Fan, F., Cai, X., Sahmani, S., Safaei, B., 2021, *Isogeometric thermal postbuckling analysis of porous FGM quasi-3D nanoplates having cutouts with different shapes based upon surface stress elasticity*, Composite Structures, 262, 113604.
66. Grygorowicz, M., Magnucki, K., Malinowski, M., 2015, *Elastic buckling of a sandwich beam with variable mechanical properties of the core*, Thin-Walled Structures, 87, pp. 127–132.
67. Ansari, R., Gholami, R., Shojaei, M.F., Mohammadi, V., Sahmani, S., 2014, *Surface stress effect on the pull-in instability of circular nanoplates*, Acta Astronautica, 102, pp. 140–150.
68. Fattahi, A.M., Safaei, B., 2017, *Buckling analysis of CNT-reinforced beams with arbitrary boundary conditions*, Microsystem Technologies, 23(10), pp. 5079–5091.
69. Liu, H., Safaei, B., Sahmani, S., 2022, *Combined axial and lateral stability behavior of random checkerboard reinforced cylindrical microshells via a couple stress-based moving Kriging meshfree model*, Archives of Civil and Mechanical Engineering, 22(1), pp. 1–20.
70. Yang, Z., Liu, A., Yang, J., Lai, S.K., Lv, J., Fu, J., 2021, *Analytical prediction for nonlinear buckling of elastically supported fg-gplrc arches under a central point load*, Materials, 14(8), pp. 1–14.
71. Yang, Z., Liu, A., Lai, S.K., Safaei, B., Lv, J., Huang, Y., Fu, J., 2022, *Thermally induced instability on asymmetric buckling analysis of pinned-fixed FG-GPLRC arches*, Engineering Structures, 250, 113243.
72. Safaei, B., Moradi-Dastjerdi, R., Behdinan, K., Chu, F., 2019, *Critical buckling temperature and force in porous sandwich plates with CNT-reinforced nanocomposite layers*, Aerospace Science and Technology, 91, pp. 175–185.
73. Magnucki, K., Magnucka-Blandzi, E., 2021, *Generalization of a sandwich structure model: Analytical studies of bending and buckling problems of rectangular plates*, Composite Structures, 255, 112944.
74. Sahmani, S., Aghdam, M.M., 2017, *Size-dependent axial instability of microtubules surrounded by cytoplasm of a living cell based on nonlocal strain gradient elasticity theory*, Journal of Theoretical Biology, 422, pp. 1339–1351.
75. Yunliang, D., Junping, H., 1995, *General buckling analysis of sandwich constructions*, Computers & Structures, 55(3), pp. 485–493.
76. Sahoo, B., Sharma, N., Mehar, K., Panda, S.K., 2020, *Numerical buckling temperature prediction of graded sandwich panel using higher order shear deformation theory under variable temperature loading* -, Smart Structures and Systems, 26, pp. 641–656.
77. Avilés, F., Carlsson, L.A., 2005, *Elastic foundation analysis of local face buckling in debonded sandwich columns*, Mechanics of Materials, 37(10), pp. 1026–1034.
78. Yuan, Y., Zhao, X., Zhao, Y., Sahmani, S., Safaei, B., 2021, *Dynamic stability of nonlocal strain gradient FGM truncated conical microshells integrated with magnetostrictive facesheets resting on a nonlinear viscoelastic foundation*, Thin-Walled Structures, 159, 107249.
79. Yang, Z., Huang, Y., Liu, A., Fu, J., Wu, D., 2019, *Nonlinear in-plane buckling of fixed shallow functionally graded graphene reinforced composite arches subjected to mechanical and thermal loading*, Applied Mathematical Modelling, 70, pp. 315–327
80. Sahmani, S., Safaei, B., 2021, *Microstructural-dependent nonlinear stability analysis of random checkerboard reinforced composite micropanels via moving Kriging meshfree approach*, The European Physical Journal Plus, 136(8), pp. 1–31.
81. Sahmani, S., Aghdam, M.M., Bahrami, M., 2016, *Size-dependent axial buckling and postbuckling characteristics of cylindrical nanoshells in different temperatures*, International Journal of Mechanical Sciences, 107, pp. 170–179.
82. Chen, S.X., Sahmani, S., Safaei, B., 2021, *Size-dependent nonlinear bending behavior of porous FGM quasi-3D microplates with a central cutout based on nonlocal strain gradient isogeometric finite element modelling*, Engineering with Computers, 37(2), pp. 1657–1678.
83. Sahmani, S., Aghdam, M.M., Rabczuk, T., 2018, *Nonlinear bending of functionally graded porous micro/nano-beams reinforced with graphene platelets based upon nonlocal strain gradient theory*, Composite Structures, 186, pp. 68–78.
84. Sahmani, S., Khandan, A., Saber-Samandari, S., Aghdam, M.M., 2018, *Nonlinear bending and instability analysis of bioceramics composed with magnetite nanoparticles: Fabrication, characterization, and simulation*, Ceramics International, 44(8), pp. 9540–9549.
85. Jasion, P., Magnucka-Blandzi, E., Szyc, W., Magnucki, K., 2012, *Global and local buckling of sandwich circular and beam-rectangular plates with metal foam core*, Thin-Walled Structures, 61, pp. 154–161.

86. Léotoing, L., Drapier, S., Vautrin, A., 2002, *First applications of a novel unified model for global and local buckling of sandwich columns*, European Journal of Mechanics-A/Solids, 21(4), pp. 683–701.
87. Fan, F., Lei, B., Sahmani, S., Safaei, B., 2020, *On the surface elastic-based shear buckling characteristics of functionally graded composite skew nanoplates*, Thin-Walled Structures, 154, 106841.
88. Sahmani, S., Aghdam, M.M., 2017, *Temperature-dependent nonlocal instability of hybrid FGM exponential shear deformable nanoshells including imperfection sensitivity*, International Journal of Mechanical Sciences, 122, pp. 129–142.
89. Ghanati, P., Safaei, B., 2019, *Elastic buckling analysis of polygonal thin sheets under compression*, Indian Journal of Physics, 93(1), pp. 47–52.
90. Yan, L.L., Han, B., Yu, B., Chen, C.Q., Zhang, Q.C., Lu, T.J., 2014, *Three-point bending of sandwich beams with aluminum foam-filled corrugated cores*, Materials & Design, 60, pp. 510–519.
91. Mehar, K., Panda, S.K., 2018, *Elastic bending and stress analysis of carbon nanotube-reinforced composite plate: Experimental, numerical, and simulation*, Advances in Polymer Technology, 37(6), pp. 1643–1657.
92. Barbaros, I., Yang, Y., Safaei, B., Yang, Z., Qin, Z., Asmael, M., 2022, *State-of-the-art review of fabrication, application, and mechanical properties of functionally graded porous nanocomposite materials*, Nanotechnology Reviews, 11(1), pp. 321–371.
93. Liu, Y., Qin, Z., Chu, F., 2020, *Analytical study of the impact response of shear deformable sandwich cylindrical shell with a functionally graded porous core*, Mechanics of Advanced Materials and Structures, 0(0), pp. 1–10.
94. Aldakheel, F., Miehe, C., 2017, *Coupled thermomechanical response of gradient plasticity*, International Journal of Plasticity, 91, pp. 1–24.
95. Aldakheel, F., 2017, *Micromorphic approach for gradient-extended thermo-elastic–plastic solids in the logarithmic strain space*, Continuum Mechanics and Thermodynamics, 29(6), pp. 1207–1217.
96. Chen, D.H., 2012, *The collapse mechanism of corrugated cross section beams subjected to three-point bending*, Thin-Walled Structures, 51, pp. 82–86.
97. Zhao, S., Zhao, Z., Yang, Z., Ke, L.L., Kitipornchai, S., Yang, J., 2020, *Functionally graded graphene reinforced composite structures: A review*, Engineering Structures, 210, 110339.
98. Wang, Y., Ermilov, V., Strigin, S., Safaei, B., 2021, *Multilevel modeling of the mechanical properties of graphene nanocomposites/polymer composites*, Microsystem Technologies, 27(12), pp. 4241–4251.
99. Zhang, J., Supernak, P., Mueller-Alander, S., Wang, C.H., 2013, *Improving the bending strength and energy absorption of corrugated sandwich composite structure*, Materials & Design, 52, pp. 767–773.
100. Alhijazi, M., Zeeshan, Q., Safaei, B., Asmael, M., Qin, Z., 2020, *Recent Developments in Palm Fibers Composites: A Review*, Journal of Polymers and the Environment, 28(12), pp. 3029–3054.
101. Alhijazi, M., Safaei, B., Zeeshan, Q., Asmael, M., Eyvazian, A., Qin, Z., 2020, *Recent developments in Luffa natural fiber composites: Review*, Sustainability, 12(18), pp. 1–25.
102. Mehar, K., Panda, S.K., 2019, *Theoretical deflection analysis of multi-walled carbon nanotube reinforced sandwich panel and experimental verification*, Composites Part B: Engineering, 167, pp. 317–328.
103. Sahmani, S., Aghdam, M.M., 2017, *Size-dependent nonlinear bending of micro/nano-beams made of nanoporous biomaterials including a refined truncated cube cell*, Physics Letters, Section A: General, Atomic and Solid State Physics, 381(45), pp. 3818–3830.
104. Safaei, B., Davodian, E., Fattahi, A.M., Asmael, M., 2021, *Calcium carbonate nanoparticles effects on cement plast properties*, Microsystem Technologies, 27(8), pp. 3059–3076.
105. Li, H., Wang, D., Xiao, Z., Qin, Z., Xiong, J., Han, Q., Wang, X., 2022, *Investigation of vibro-impact resistance of fiber reinforced composite plates with polyurea coating with elastic constraints*, Aerospace Science and Technology, 121, 107196.
106. Seong, D.Y., Jung, C.G., Yang, D.Y., Ahn, J., Na, S.J., Chung, W.J., Kim, J.H., 2010, *Analysis of core shear stress in welded deformable sandwich plates to prevent de-bonding failure during U-bending*, Journal of Materials Processing Technology, 210(9), pp. 1171–1179.
107. Mehar, K., Panda, S.K., Patle, B.K., 2018, *Stress, deflection, and frequency analysis of CNT reinforced graded sandwich plate under uniform and linear thermal environment: A finite element approach*, Polymer Composites, 39(10), pp. 3792–3809.
108. Fattahi, A.M., Safaei, B., Qin, Z., Chu, F., 2021, *Experimental studies on elastic properties of high density polyethylene-multi walled carbon nanotube nanocomposites*, Steel and Composite Structures, An International Journal, 38(2), pp. 177–187.
109. Sivaram, A.R., Manikandan, N., Krishnakumar, S.K., Rajavel, R., Krishnamohan, S., Vijayaganth, G., 2020, *Experimental study on aluminium based sandwich composite with polypropylene foam sheet*, Materials Today: Proceedings, 24, pp. 746–753.

110. Hu, J.S., Wang, B.L., 2021, *Crack growth behavior and thermal shock resistance of ceramic sandwich structures with an auxetic honeycomb core*, Composite Structures, 260, 113256.
111. Daouas, N., Hassen, Z., Aissia, H. Ben, 2010, *Analytical periodic solution for the study of thermal performance and optimum insulation thickness of building walls in Tunisia*, Applied Thermal Engineering, 30(4), pp. 319–326.
112. Wang, X., Wang, Z., Zeng, T., Cheng, S., Yang, F., 2018, *Exact analytical solution for steady-state heat transfer in functionally graded sandwich slabs with convective-radiative boundary conditions*, Composite Structures, 192, pp. 379–386.
113. Geoffroy, L., Davesne, A., Bellayer, S., Blanchard, F., Richard, E., Samyn, F., Jimenez, M., Bourbigot, S., 2020, *3D printed sandwich materials filled with hydrogels for extremely low heat release rate*, Polymer Degradation and Stability, 179, 109269.
114. Safaei, B., Onyibo, E.C., Hurdoganoglu, D., 2022, E*ffect of static and harmonic loading on the honeycomb sandwich beam by using finite element method*, Facta Universitatis, Series: Mechanical Engineering, doi: 10.22190/FUME220201009S
115. Patil, S.P., Parale, V.G., Park, H.H., Markert, B., 2021, *Mechanical modeling and simulation of aerogels: A review*, Ceramics International, 47(3), pp. 2981–2998.
116. Ogasawara, T., Ayabe, S., Ishida, Y., Aoki, T., Kubota, Y., 2018, *Heat-resistant sandwich structure with carbon fiber-polyimide composite faces and a carbon foam core*, Composites Part A: Applied Science and Manufacturing, 114, pp. 352–359.
117. Bekuit, J.-J.R.B., Oguamanam, D.C.D., Damisa, O., 2007, *A quasi-2D finite element formulation for the analysis of sandwich beams*, Finite Elements in Analysis and Design, 43(14), pp. 1099–1107.
118. Lecturer, S., 1969, Front Matter, *Analysis and Design of Structural Sandwich Panels*, doi: 10.1016/b978-0-08-012870-2.50015-8
119. Fleck, N.A., Sridhar, I., 2002, *End compression of sandwich columns*, Composites - Part A: Applied Science and Manufacturing, 33(3), pp. 353–359.
120. Goswami, P., Student, M.E., Indore, R., Pradesh, M., 2018, *Thermal Insulation analysis of an Aramid honeycomb Sandwich Structure Filled with Silica Aerogel*, International Journal of Engineering Research in Mechanical and Civil Engineering, 3(7), pp. 1–6.